Journal of Applied Polymer Science

Influence of magnesium sulfate whiskers on the structure and properties of melt-stretching polypropylene microporous membranes

Caihong Lei, Qi Cai, Ruijie Xu, Xiande Chen, Jiayi Xie
Guangdong Provincial Key Laboratory of Functional Soft Condensed Matter, School of Materials and Energy, Guangdong University of Technology, Guangzhou 510006, People's Republic of China
Correspondence to: C. Lei (E-mail: lch528@gdut.edu.cn)

ABSTRACT: The influence of magnesium sulfate ($MgSO_4$) whiskers on the structure and properties of polypropylene cast films and stretched microporous membranes was investigated. We found that for the cast films, $MgSO_4$ showed some nucleation effects, and the introduction of $MgSO_4$ led to the decrease of the orientation degree along the machine direction (MD), whereas that along the transverse direction (TD) was improved; this indicated that $MgSO_4$ whiskers were mainly arranged along the TD. The introduction of $MgSO_4$ up to 10 wt % did not induce apparent changes in the pore structure and air permeability properties of the stretched microporous membranes but improved the electrolyte absorption ability. The most pronounced change for the stretched microporous membranes was the strength along the TD. It was increased by 110% when the $MgSO_4$ content was 2 wt %. During the fabrication of microporous membranes, only stretching along the MD was carried out to initiate pore formation; this resulted in a lower strength along the TD. This study gave us a method for improving the mechanical properties of stretched microporous membranes along the TD. The obtained microporous membranes with better electrolyte absorption and higher mechanical strength along the TD could be used in lithium-ion batteries as separators. © 2016 Wiley Periodicals, Inc. J. Appl. Polym. Sci. **2016**, *133*, 43884.

KEYWORDS: composites; crystallization; differential scanning calorimetry (DSC)

Received 3 January 2016; accepted 29 April 2016
DOI: 10.1002/app.43884

INTRODUCTION

Functional microporous membranes have been widely used in fields such as filtration,[1] separation,[2] and new energy[3] and especially in the field of lithium-ion batteries as separators. Usually, microporous separators can be fabricated on the basis of thermally induced phase separation, polypropylene (PP) crystal transformation, and melt-stretching mechanisms.[4–6] Compared with the former two methods, the melt-stretching method is more environmentally friendly and shows better pore structure control. This process mainly covers four stages[7,8]: (1) the production of the precursor film with a row-nucleated lamellar morphology; (2) annealing to thicken the lamellae and obtain a hard elastic film, which shows a higher elastic recovery; (3) the stretching of the film at low temperature to create voids and then stretching at a high temperature to enlarge the pores, and (4) heat setting to improve the dimensional stability. During the whole process, only stretching along the machine direction (MD) is carried out; this results in a lower strength along the transverse direction (TD) and some surface defects, such as waves and bands. Bioriented stretching is carried out for the membranes prepared on the basis of thermally induced phase separation and the crystal transformation mechanism. Hence, compared with these membranes, the most important disadvantage of separators based on the melt-stretching method is its lower strength along the TD.

To improve the mechanical properties along the TD for PP microporous membranes prepared by the melt-stretching method, in our previous study, the microporous membranes were first prepared, and then, transverse stretching was carried out. We found that the yield strength was improved by only 17% after stretching by 10%. Stretching of 35% led to pronounced deterioration of the pore structure.[9] Therefore, it is necessary to look for other methods to improve the strength without the deterioration of the pore structure.

As one kind of filler with a one-dimensional structure, inorganic whiskers are often added to polymers with the aim of enhancing their mechanical properties.[10–12] The tensile strength of PP/whisker composites with a whisker content of 10 wt % was found to be improved by 56%.[13] In addition, magnesium sulfate ($MgSO_4$) whiskers can be used as fire retardants in polymer and rubber systems, and they can also improve the thermal stability.[14,15] In our previous work, we found that when silicone dioxide was added to PP, microporous membranes with a larger pore diameter, better air permeability, and higher tensile

strength along the MD were obtained.[16] Recently, some new experiments have shown that the introduction of some $MgSO_4$ did not show a pronounced influence on the air permeability properties of PP microporous membranes. At the same time, it led to an increase in their strength along the TD. In this study, we investigated the influence of the $MgSO_4$ whisker content on the crystalline structure of PP precursor films and the properties of stretched microporous membranes. Also, we provide an easy method for improving the TD strength of microporous membranes fabricated on the basis of the melt-stretching mechanism.

EXPERIMENTAL

Materials

A homo-PP resin with a melt flow rate value of 2.0 g/10 min (230 °C and 2.16 kg) from Yangzi Petrochemical Co. (China) was used. The weight-average molecular weight and polydispersity index were about 754 kg/mol and 6.29, respectively. The melting peak point and the crystallinity obtained from differential scanning calorimetry (DSC; PerkinElmer DSC 7, Waltham, MA) at a rate of 10 °C/min, were 164.2 °C and 39.0%, respectively. The reported crystallinity results were obtained with a heat of fusion of 209 J/g for a fully crystalline PP.[17]

$MgSO_4$ whiskers were supplied by Shanghai Muhong Industrial Co., Ltd. (China). Figure 1 shows their microstructure. The length-to-diameter ratio was around 20.

Preparation of Cast Films and Stretched Microporous Membranes

First, the masterbatch with the $MgSO_4$ content of 10 wt % was prepared with a twin-screw extruder by Brabender Co. (Germany). Then, the masterbatch was blended with PP to prepare the compound with different contents of $MgSO_4$ in an internal mixer from Dongguan Lina Machine Co. (China). The precursor cast films, which included different contents of $MgSO_4$ (0, 0.5, 1, 2, 5, and 10 wt %) were prepared by cast extrusion through a T-slot die. During this process, the uniaxial (MD) stretching was applied to the compound melt. The die temperature was set at 220 °C, and a draw ratio of 106 was applied. The draw ratio was determined by the take-up speed because the extruded velocity at the exit of the die was constant. The chill roll temperature was set at 80 °C. The thickness of the precursor films was controlled at around 20 μm.

Then, annealing was carried out in a hot oven at 145 °C for 30 min. An Instron 3365 machine equipped with a heating chamber was used for the room-temperature and hot stretching. The annealed films were first stretched to 15% at room temperature and then stretched to 100% at 130 °C. A drawing speed of 50 mm/min was applied during room-temperature and hot stretching. After stretching, the films were heat-set at 145 °C for 10 min to improve the dimensional stability.

Characterization

The orientation degree of the samples was characterized by Fourier transform infrared (FTIR) spectroscopy. The spectra were recorded on a Nicolet 6700 FTIR instrument from Thermo Electron Corp. with a resolution of 4/cm. The beam was polarized by means of a Spectra-Tech zinc selenide wire grid polarizer from Thermo Electron Corp. The dichroic ratio (R) was calculated by the ratio of the absorbance from beams polarized parallel to the melt extrusion direction ($A_{\parallel}$) to the absorbance from beams polarized perpendicular to the melt extrusion direction ($A_{\perp}$). Then, the data were evaluated with the degree of orientation:[18]

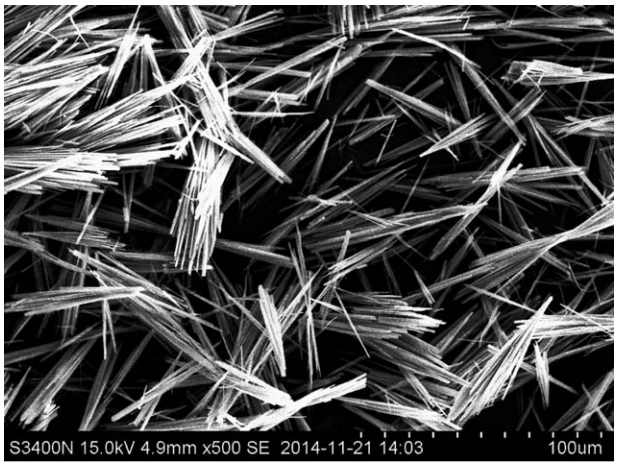

Figure 1. Microstructure of the $MgSO_4$ whiskers.

$$R = \frac{A_{\parallel}}{A_{\perp}} \tag{1}$$

$$f = \frac{R-1}{R+2} \times \frac{R_0+2}{R_0-1} \tag{2}$$

R_0 is the dichroic ratio of the polymer chain axis was given by

$$R_0 = 2\cot^2\Psi \tag{3}$$

where Ψ is the angle between the polymer chain axis and the transition moment of the investigated absorption band. For PP, the absorption at the wave number of 998 cm^{-1} was attributed to the crystalline phase (c axis), and the orientation of the crystalline phase (f_c) was determined. The absorption at 972 cm^{-1} was due to the contribution of both crystalline and amorphous phases, and the average orientation function (f_{av}) was obtained. Then, the orientation of the amorphous phase (f_a) was obtained from the following relation:

$$f_{av} = X_c f_c + (1-X_c) f_a \tag{4}$$

where X_c is the crystallinity as determined with a DSC test.

The melting and crystalline behaviors were observed with DSC (PerkinElmer DSC-7, PerkinElmer, Inc.). The temperature was raised from 80 to 230 °C at a rate of 5 °C/min under a nitrogen atmosphere. X_c was calculated as follows:

$$X_c = \frac{\Delta H}{\Delta H^0} \times \frac{1}{Wt} \times 100\% \tag{5}$$

where ΔH is the measured value of the fusion enthalpy, ΔH^0 is the fusion enthalpy of perfectly crystalline PP (i.e., 209 J/g), and Wt is the mass fraction of PP.[17]

The thermogravimetry (TG) curve was obtained with a thermal gravity analyzer (SDT-2960, TA Instruments) from 80 to 580 °C at a rate of 10 °C/min under a nitrogen atmosphere.

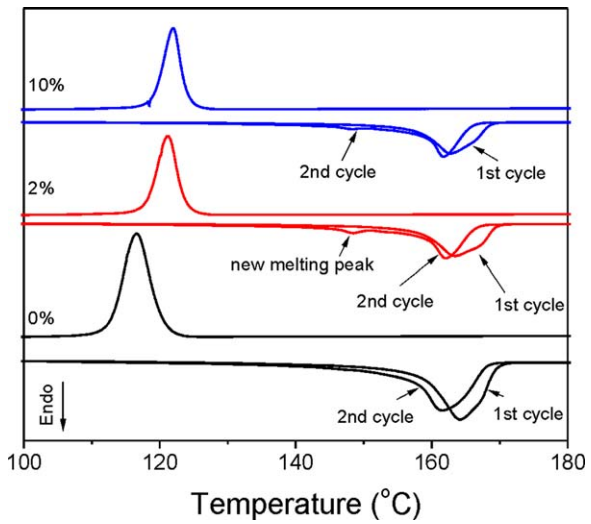

Figure 2. DSC curves of the PP/$MgSO_4$ cast films with $MgSO_4$ contents of 0, 2, and 10 wt %. [Color figure can be viewed in the online issue, which is available at wileyonlinelibrary.com.]

The elastic recovery of the cast films was tested with an Instron 3365 machine along the MD at a deformation rate of 50 mm/min. The elastic recovery (%) was calculated with the following equation:

$$\text{Elastic recovery } (\%) = (L-L')/(L-L_0) \times 100\% \qquad (6)$$

where L_0, L, and L' are the initial length of the film before extension, the length when it is strained to 100%, and the length at the end of extension, respectively.

The surface morphology was characterized by scanning electron microscopy (SEM; S3400-N, Hitachi, Japan). All of the samples were sputtered with a platinum ion beam for 300 s before testing.

According to ASTM D 726, a Gurley densometer (model 4150, Gurley Precision Instruments, New York) was used to characterize the air permeability of the microporous membranes. The Gurley value was defined as the time required for 100 mL of air to pass through a specific area under 20 kgf/cm^2.[19] The low Gurley value corresponded to a high air permeability. According to ASTM D 2873, the porosity was measured with liquid absorption methods. Paraffin oil was used, and the porosity was calculated on the basis of the weight difference before and after immersion in the liquid.

The mechanical properties along the MD and TD were tested with an Instron 3365 machine. During the tensile tests, a strain rate of 50 mm/min was used.

To measure the electrolyte uptake, the stretched microporous membrane was soaked in the liquid electrolyte for 12 h, and then, the ratio of weight gain to the dry membrane was calculated.

RESULTS AND DISCUSSION

Influence of the $MgSO_4$ Content on the Orientation and Crystalline Properties of the Initial Cast Films

It is known that the crystalline structure in the initial cast films determines the pore structure of stretched microporous membranes. To characterize the crystalline structural changes induced by $MgSO_4$, the orientation degree and crystalline properties were tested.

The effect of $MgSO_4$ on the PP crystallization was characterized by a two-cycle DSC heating experiment. Figure 2 shows the DSC curves of the PP/$MgSO_4$ cast films with $MgSO_4$ contents of 0, 2, and 10 wt %. The first heating cycle was used to remove the effect of the internal stress and the molecular orientation on the melting enthalpy calculation. During the cooling process, the crystallization behavior was only affected by the cooling rate and the contents of $MgSO_4$. The effect of $MgSO_4$ on PP crystallization is shown during the secondary heating cycle. The temperature of the crystalline peak was moved to a higher temperature by $MgSO_4$, and for compound films, a weak new melting peak appeared before the main melting peak during the secondary heating scan; this indicated that $MgSO_4$ showed some nucleation effects in the compound films. The crystallinities of PP/$MgSO_4$ cast films with different contents of $MgSO_4$ were calculated with eq. (5) and are listed in Table I. The crystallinity of the compound films gradually increased with increasing content of $MgSO_4$. The results show that the $MgSO_4$ whiskers acted as a nucleating agent.

Figure 3 shows the polarized FTIR spectra of the PP/$MgSO_4$ cast films with $MgSO_4$ contents of 0, 2, and 10 wt % along the MD and TD. The particular peak at 998 cm^{-1} was related to the crystalline phase, and the peak at 972 cm^{-1} was due to the contributions of both the crystalline and amorphous phases. The 0 and 90° indicate that the polarizer was parallel and vertical, respectively, to the MD.[16] On the basis of eqs. (1–4), f_c, f_a, and f_{av} were calculated.

Figure 4 shows the orientation degree of the PP/$MgSO_4$ cast films along the MD and TD with different contents of s$MgSO_4$. The introduction of $MgSO_4$ led to decreases in f_c, f_a, and f_{av} along the MD. f_c decreased from 0.38 to 0.33 with increasing $MgSO_4$ content from 0 to 2 wt %. Then, the degree did not change much at higher $MgSO_4$ contents. However, it was surprising that f_{av} along the TD was improved from 0.06 without $MgSO_4$ to 0.39 when the $MgSO_4$ content was 2 wt %. The low orientation degree along the TD for the pure PP cast film was acceptable because the cast film was prepared by melt stretching only along the MD. The improvement in the orientation degree along the TD indicated that under the melt-stretching field, the $MgSO_4$ whiskers in the compound cast film were mainly arranged along the TD.

For the preparation of PP microporous membranes based on the melt-stretching mechanism, it is well known that precursor films with a row-nucleated crystalline structure must be prepared first, and this kind of crystalline structure decides the

Table I. Crystallinities of PP/$MgSO_4$ Cast Films with Different Contents of $MgSO_4$

	$MgSO_4$ content (wt %)					
	0	0.5	1	2	5	10
Crystallinity (%)	40.1	42.0	45.6	46.7	45.2	44.3

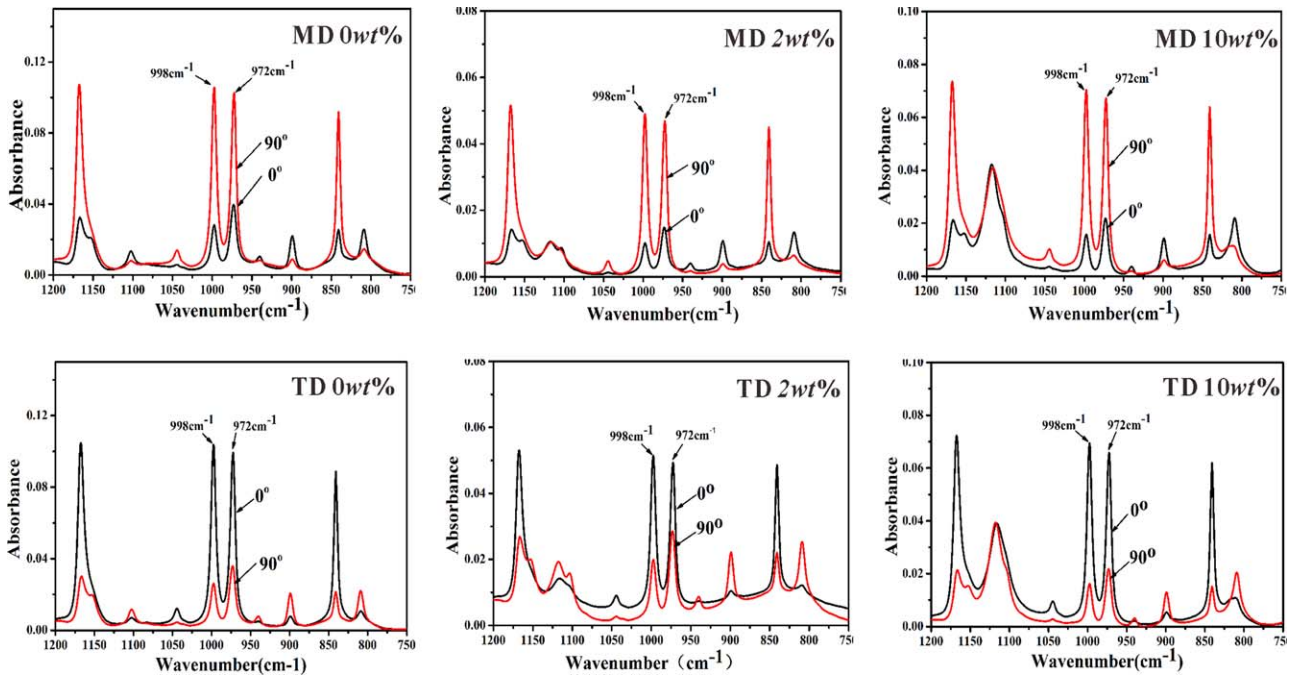

Figure 3. Polarized FTIR spectra of PP/$MgSO_4$ with $MgSO_4$ contents of 0, 2, and 10 wt % in the range 1200–750 cm^{-1} along the MD and TD. [Color figure can be viewed in the online issue, which is available at wileyonlinelibrary.com.]

pore formation and size in the finally stretched microporous membranes.[20–22] To obtain this kind of crystalline structure, the elongational stress is applied to the melt during the cast process. Here, the matching of the orientation and material crystalline ability was very important. The nucleation effect of $MgSO_4$ may have broken the matching of the orientation and crystalline rate during the preparation of the initial cast films, and this resulted in a deformed lamellae crystalline structure in the compound films. The formation of the deformed lamellae resulted in a decrease in the orientation degree along the MD. However, it was apparent that compared with the increase in the orientation degree along the TD, the decrease in the orientation degree along the MD was small.

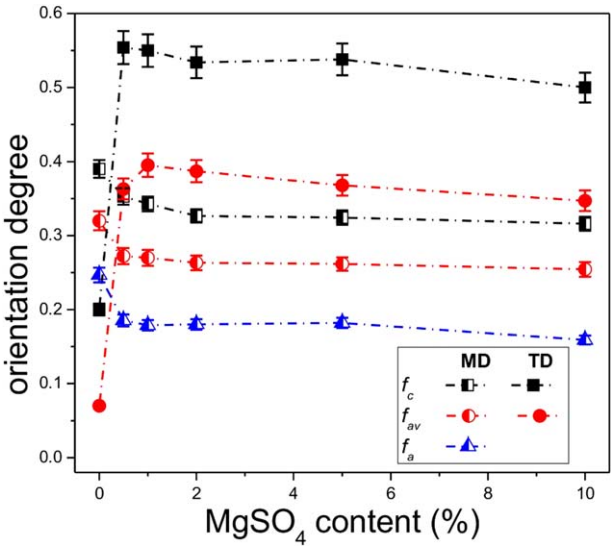

Figure 4. f_c, f_{av}, and f_a along the MD and f_c and f_{av} along the TD of the PP/$MgSO_4$ cast films with different contents of $MgSO_4$. [Color figure can be viewed in the online issue, which is available at wileyonlinelibrary.com.]

The precursor films with a row-nucleated crystalline structure showed a hard elastic behavior. Table II lists the elastic recovery values of the compound films with different contents of $MgSO_4$. With increasing $MgSO_4$ content to 2 wt %, the elastic recovery was about 85.6%; this was 1% less than that of the pure PP film. When the $MgSO_4$ content was higher than 5 wt %, the elastic recovery only decreased to 83.4% and still showed a higher hard elastic behavior. It was apparent that the previous decrease in the orientation degree along the MD did not show a pronounced effect on the elastic recovery behavior.

Influence of the $MgSO_4$ Content on the Pore Structure and Properties of the Stretched Microporous Membranes

Figure 5 shows the SEM morphology of PP/$MgSO_4$ microporous membranes with different contents of $MgSO_4$. No apparent interfacial pores between PP and $MgSO_4$ were found. In contrast, pores surrounded by bridges connecting the separated lamellae were observed for all of the membranes. This indicated that here the pores were mainly from the separation of the lamellae structure during the first stretching at room

Table II. Elastic Recovery Values of PP/$MgSO_4$ Cast Films with Different Contents of $MgSO_4$

	$MgSO_4$ content (%)					
	0	0.5	1	2	5	10
Elastic recovery (%)	86.6	86.4	86.4	85.6	83.4	83.4

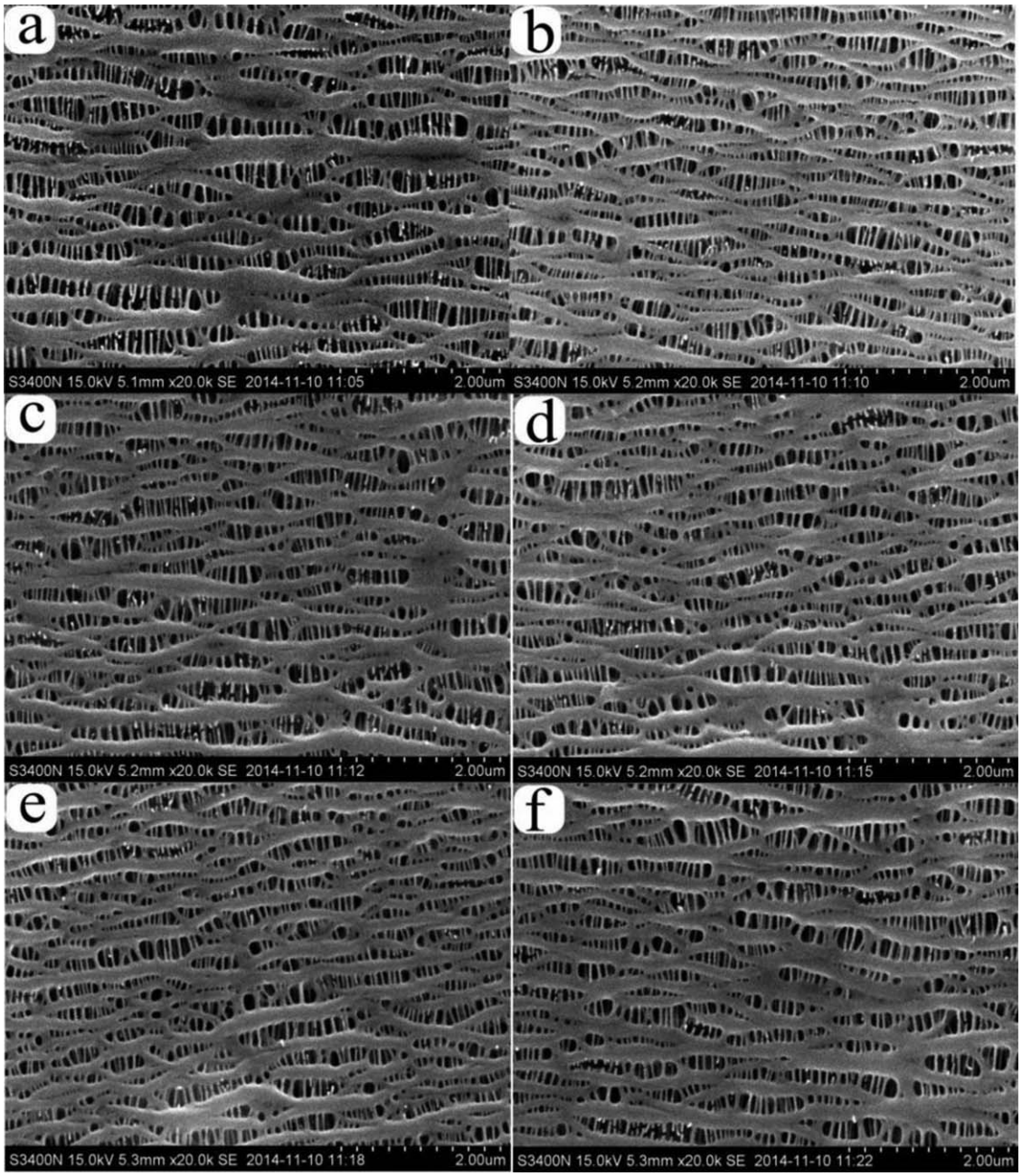

Figure 5. SEM images of PP/$MgSO_4$ microporous membranes with different contents of $MgSO_4$: (a) 0, (b) 0.5, (c) 1, (d) 2, (e) 5, and (f) 10 wt %.

temperature and then during stretching at 130 °C. The introduction of $MgSO_4$ did not induce apparent changes in the pore formation mechanism.

To prove the existence of $MgSO_4$ in the stretched microporous membranes, we tested TG curves of the pure PP and PP/$MgSO_4$ compound microporous membranes with an $MgSO_4$ content of 10 wt %, and these are shown in Figure 6. We observed that the introduction of $MgSO_4$ improved the thermal stability. For pure PP membrane, the mass percentage at a temperature of 500 °C was about 0%, whereas the compound membrane showed a mass percentage of about 10 wt %; this proved the existence of $MgSO_4$ in the compound membrane.

Table III lists the Gurley values and porosities of PP/$MgSO_4$ microporous membranes with different contents of $MgSO_4$. Compared with that of the membrane without $MgSO_4$, the porosity of the compound membranes was decreased by 1.9% to 4.1%, and the corresponding Gurley value was increased by 10–20 s. The whole change was not pronounced. The Gurley value of the membrane with an $MgSO_4$ content of 10 wt % was still acceptable for its application in the field of lithium-ion batteries as a separator. It has been reported that the higher the elastic recovery of initial film is, the lower the Gurley value is and the better the air permeability is.[16] The introduction of $MgSO_4$ of 10 wt % only led to a decrease of elastic recovery

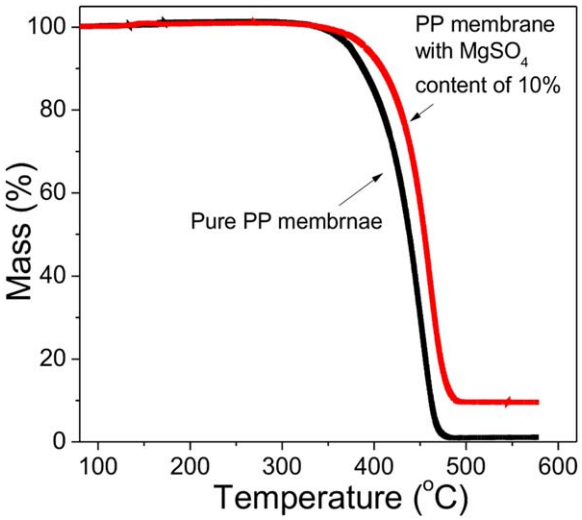

Figure 6. TG curves of the pure PP and PP/$MgSO_4$ microporous membranes with $MgSO_4$ contents of 10 wt %. [Color figure can be viewed in the online issue, which is available at wileyonlinelibrary.com.]

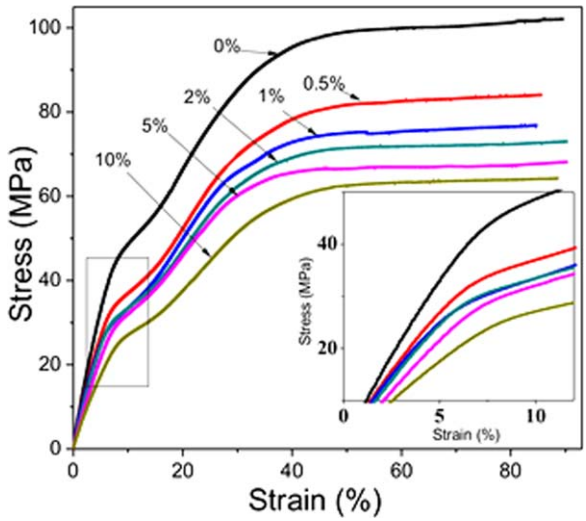

Figure 7. Stress–strain curves along the MD of PP/$MgSO_4$ microporous membranes with different contents of $MgSO_4$. [Color figure can be viewed in the online issue, which is available at wileyonlinelibrary.com.]

from 86.6 to 83.5%; hence, the pore properties of the stretched microporous membranes were not influenced pronouncedly.

Influence of the $MgSO_4$ Content on the Mechanical Properties of the Stretched Microporous Membranes

Figure 7 presents the stress–strain curves of PP/$MgSO_4$ microporous membranes with different contents of $MgSO_4$ along the MD. It was surprising that with increasing $MgSO_4$ content, the curve showed a lower yield strength and elastic modulus. The elastic modulus (the curve of the slope before the yield point) of the membrane without $MgSO_4$ was 638.1 MPa. The corresponding value at an $MgSO_4$ content of 10 wt % decreased to 340.5 MPa. The yield strength and breaking strength are shown in Table IV. With increasing $MgSO_4$ content to 10 wt %, the yield strength and break strength decreased by 42.7 and 37.1%, respectively.

Figure 8 shows the stress–strain curves along the TD of PP/$MgSO_4$ microporous membranes with different contents of $MgSO_4$. It was also surprising to find that with increasing $MgSO_4$ content to 2 wt %, the yield strength increased by 110% from 7.8 to 16.4 MPa. A further increase in the $MgSO_4$ content to 10 wt % led to a decrease in the yield strength. The most important disadvantage of the PP microporous membranes based on the melt-stretching mechanism was its lower strength along the TD, which was due to the stretching only along the MD during the fabrication. Here, the results show that the introduction of $MgSO_4$ afforded a method for improving the mechanical properties along the TD for PP microporous membranes.

To explain the change in the mechanical properties, the orientation degrees of stretched microporous membranes with $MgSO_4$ contents of 0, 2, and 10 wt % along the MD and TD were tested and are shown in Figure 9. Along the MD, the f_{av} values were 0.26, 0.28 and 0.30, respectively. It was apparent that $MgSO_4$ led to a small increase in the orientation degree along the MD in the microporous membrane. During stretching, as one kind of filler, $MgSO_4$ may have promoted the orientation and induced the increase in the orientation degree. In our previous work,[16] we also found that the introduction of 2 wt % silicon dioxide led to an increase in the orientation degree of the stretched PP microporous membranes from 0.28 to 0.34. In addition, as shown in Figure 9, along the TD, the f_{av} value of the pure PP membrane was only 0.08; this was far less than that along the MD. However, the introduction of $MgSO_4$ led to a pronounced increase in the orientation degree, and when the $MgSO_4$ content was 2 wt %, the orientation degree increased to 0.30. This further proved that the whiskers were mainly

Table III. Properties of PP/$MgSO_4$ Microporous Membranes with Different Contents of $MgSO_4$

	$MgSO_4$ content (wt %)					
	0	0.5	1	2	5	10
Gurley value (s/100 mL)	230	242	247	240	246	250
Porosity (%)	52.1	49.9	48.8	50.2	48.9	48.0

Table IV. Mechanical Properties of PP/$MgSO_4$ Microporous Membranes with Different Contents of $MgSO_4$

	$MgSO_4$ content (wt %)					
	0	0.5	1	2	5	10
Yield strength along MD (MPa)	43.3	32.3	26.1	25.6	25.0	24.8
Break strength along MD (MPa)	102.1	84.1	75.3	73.0	68.2	64.2
Yield strength along TD (MPa)	7.8	12.3	14.5	16.4	10.1	4.7
Break strength along TD (MPa)	6.7	12.6	13.4	15.9	9.7	4.5

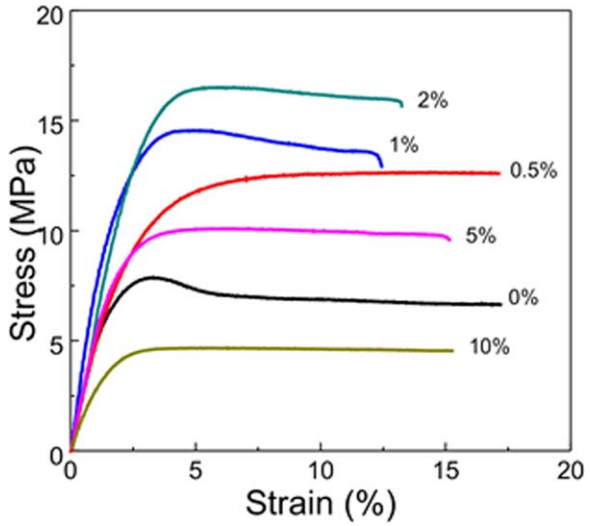

Figure 8. Stress–strain curves along the TD of PP/$MgSO_4$ microporous membranes with different contents of $MgSO_4$. [Color figure can be viewed in the online issue, which is available at wileyonlinelibrary.com.]

arranged along the TD in the stretched microporous membranes. This explained the increase in the yield strength along the TD. When the $MgSO_4$ content was 10 wt %, the corresponding yield strength decreased. This may have been due to the existence of some agglomerates in the compound membrane. The whiskers were arranged along the TD. During stretching along the MD, the previous result shows that the yield strength was decreased for the compound membranes. This may have been due to the weak interface between $MgSO_4$ and PP because, in this experiment, $MgSO_4$ was used without surface treatment.

Influence of the $MgSO_4$ Content on the Electrolyte Uptake of Stretched Microporous Membranes

For the pure PP microporous membranes, because of their hydrophobicity, when they were used in lithium-ion batteries as separators, the most important disadvantages were their lower electrolyte absorption and retention. Figure 10 shows the electrolyte uptake values of PP/$MgSO_4$ microporous membranes with $MgSO_4$ contents of 0, 1, 5, and 10 wt %. It was apparent that the introduction of $MgSO_4$ induced the improvement of the electrolyte uptake of PP microporous membranes.

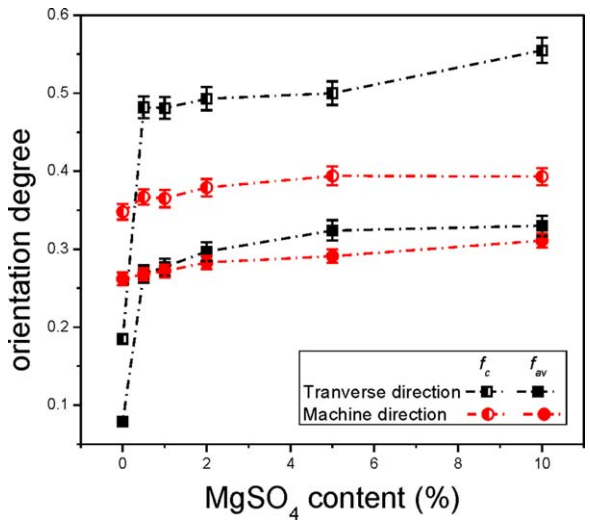

Figure 9. Orientation degree of microporous membranes with different contents of $MgSO_4$ along the MD and TD. [Color figure can be viewed in the online issue, which is available at wileyonlinelibrary.com.]

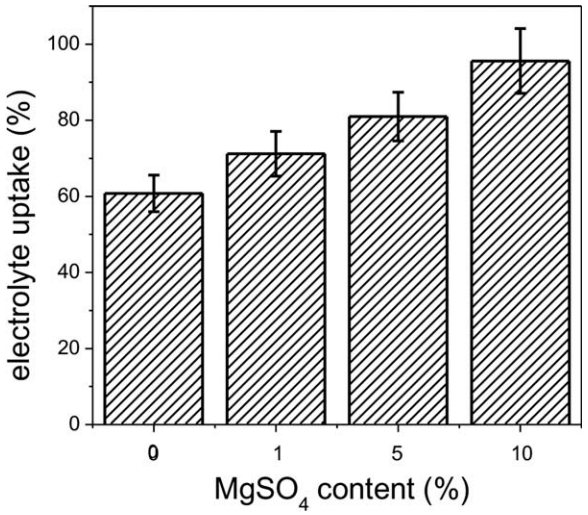

Figure 10. Electrolyte uptake of PP/$MgSO_4$ microporous membranes with $MgSO_4$ contents of 0, 1, 5, and 10 wt %.

CONCLUSIONS

The effects of $MgSO_4$ whiskers on the structure and properties of PP microporous membranes prepared on the basis of the melt-stretching mechanism were investigated. With increasing $MgSO_4$ content to 10 wt %, the f_c value of the initial precursor film along the MD decreased from 0.38 to 0.32, whereas that along the TD increased from 0.20 to 0.50. The porosity of the stretched microporous membranes decreased by 4.1%, whereas the Gurley value only increased by 20 s. The introduction of $MgSO_4$ up to 10 wt % did not induce pronounced changes in the pore structure and air permeability properties of the stretched microporous membranes; at the same time, it induced the improvement of the electrolyte uptake. It was surprising to find that the strength along the MD was decreased by $MgSO_4$, whereas that along the TD was apparently increased by 110% when the $MgSO_4$ content was 2 wt % because the $MgSO_4$ whiskers were mainly arranged along the TD in the compound membranes. This study indicated that a small content of $MgSO_4$ could lead to an increase in the mechanical properties along the TD for PP microporous membranes; at the same time, it did not deteriorate the pore structure and air permeability properties.

ACKNOWLEDGMENTS

The authors thank the National Science Foundation of China (contract grant number 51003017) and the Project of High Level Talents in Higher School of Guangdong Province for their financial support. They also thank Shenzhen Senior Materials Co., Ltd., for generously supplying raw materials.

REFERENCES

1. Elisabete, C.; Alexandros, S. *Compos. Sci. Technol.* **2012**, *72*, 799.
2. Ge, B.; Zhang, Z.; Zhu, X.; Men, X.; Zhou, X.; Xue, Q. *Compos. Sci. Technol.* **2014**, *102*, 100.
3. Xu, R.; Chen, X.; Xie, J.; Cai, Q.; Lei, C *Ind. Eng. Chem. Res.* **2015**, *54*, 2991.
4. Tang, N.; Jia, Q.; Zhang, H.; Li, J.; Cao, D. *Desalination* **2010**, *256*, 27.
5. Dai, J.; Liu, X.; Yang, J.; Zhang, N.; Huang, T.; Wang, Y.; Zhou, Z. *Compos. Sci. Technol.* **2014**, *99*, 59.
6. Xu, R.; Lei, C.; Cai, Q.; Hu, B.; Shi, W.; Mo, H.; Chen, C. *Plast. Rubber Compos.* **2014**, *43*, 257.
7. Castro, A. J. U.S. Pat. 4,247,498 (**1981**).
8. Funaoka, H.; Kaimai, N.; Kono, K. U.S. Pat. 6,153,133, (**2000**).
9. Cai, Q.; Lei, C.; Xu, R.; Hu, B. *Mater. Res. Appl.* **2014**, *15*, 8.
10. Xia, Y.; Yang, P.; Sun, Y. *Adv. Mater.* **2003**, *15*, 353.
11. Lu, H.; Hu, Y.; Yang, L. *Macromol. Mater. Eng.* **2004**, *289*, 984.
12. Chang, Z.; Guo, F.; Yu, J. *Polym. Mater. Sci. Eng.* **2006**, *22*, 217.
13. Gao, C.; Wang, T.; Xu, L. J. *Chem. Eng. Chin. Univ.* **2014**, *28*, 143.
14. Fang, S.; Hu, Y.; Son, L.; Zhan, J.; He, Q. *J. Mater. Sci.* **2008**, *43*, 1057.
15. Liu, B.; Zhang, Y.; Wan, C.; Zhang, Y.; Li, R.; Liu, G. *Polym. Bull.* **2007**, *58*, 747.
16. Cai, Q.; Xu, R.; Chen, X.; Chen, C.; Mo, H.; Lei, C. *Polym. Compos.* **2015**, DOI: 10.1002/pc.23462.
17. Sadeghi, F.; Ajji, A.; Carreau, P. J. *Proc. Soc. Plast. Eng. Annu. Tech. Conf.* **2005**, *1*, 163.
18. Houska, M.; Brummell, M. *Polym. Eng. Sci.* **1987**, *27*, 917.
19. Taskier, H. T. U.S. Pat. 4,359,510 (**1982**).
20. Tabatabaei, S. H.; Carreau, P. J.; Ajji, A. *J. Membr. Sci.* **2009**, *345*, 148.
21. Lee, S. Y.; Park, S. Y.; Song, H. S. *J. Appl. Polym. Sci.* **2007**, *103*, 3326.
22. Tabatabaei, S. H.; Carreau, P. J.; Ajji, A. *Polymer* **2009**, *50*, 4228.